Published online July 14, 2004

3712–3723 *Nucleic Acids Research, 2004, Vol. 32, No. 12*
doi:10.1093/nar/gkh696

Biological consequences of oxidative stress-induced DNA damage in *Saccharomyces cerevisiae*

Tiffany B. Salmon[1,2], Barbara A. Evert[1,2], Binwei Song[1] and Paul W. Doetsch[3,*]

[1]Department of Biochemistry, [2]Graduate Program in Genetics and Molecular Biology and [3]Department of Biochemistry and Division of Cancer Biology and Department of Radiation Oncology, Emory University School of Medicine, Atlanta, GA 30322, USA

Received April 30, 2004; Revised June 11, 2004; Accepted June 21, 2004

ABSTRACT

Reactive oxygen species (ROS), generated by endogenous and exogenous sources, cause significant damage to macromolecules, including DNA. To determine the cellular effects of induced, oxidative DNA damage, we established a relationship between specific oxidative DNA damage levels and biological consequences produced by acute H_2O_2 exposures in yeast strains defective in one or two DNA damage-handling pathways. We observed that unrepaired, spontaneous DNA damage interferes with the normal cellular response to exogenous oxidative stress. In addition, when base excision repair (BER) is compromised, there is a preference for using recombination (REC) over translesion synthesis (TLS) for handling H_2O_2-induced DNA damage. The global genome transcriptional response of these strains to exogenous H_2O_2 exposure allowed for the identification of genes responding specifically to induced, oxidative DNA damage. We also found that the presence of DNA damage alone was sufficient to cause an increase in intracellular ROS levels. These results, linking DNA damage and intracellular ROS production, may provide insight into the role of DNA damage in tumor progression and aging. To our knowledge, this is the first report establishing a relationship between H_2O_2-induced biological endpoints and specific oxidative DNA damage levels present in the genome.

INTRODUCTION

Reactive oxygen species (ROS), such as the superoxide radical, hydroxyl radical and H_2O_2, pose a significant threat to cellular integrity in terms of damage to DNA, lipids, proteins and other macromolecules (1,2). ROS are generated through both endogenous and exogenous routes. The majority of endogenous ROS are produced through leakage of these species from the mitochondrial electron transport chain (3). In addition, cytosolic enzyme systems, including NADPH oxidases, and by-products of peroxisomal metabolism are also endogenous sources of ROS. Generation of ROS also occurs through exposure to numerous exogenous agents and events including ionizing radiation (IR), UV, cytokines, growth factors, chemotherapeutic drugs, environmental toxins, hyperthermia and macrophages during the inflammatory response (3,4). Given the broad range of ROS sources and the highly reactive nature of many of these species, it is not surprising that ROS have been implicated in a number of disease states (1,2). Elevated levels of ROS have been implicated in the etiology of cancer, neurodegenerative and cardiovascular disease as well as the aging process (2,3,5). In addition, elevated ROS in breast cancer cells has been proposed as a condition promoting metastasis (6).

Oxidative damage, produced by intracellular ROS, results in DNA base modifications, single- and double-strand breaks, and the formation of apurinic/apyrimidinic lesions, many of which are toxic and/or mutagenic (7). Therefore, not only are ROS implicated in the etiology of disease states, but the resulting DNA damage may also be a direct contributor to deleterious biological consequences. Mutagenic 8-hydroxyguanine lesions are present in elevated levels in aged and cancer cells. In addition, H_2O_2-induced oxidative DNA damage has been shown to cause microsatellite instability, which is associated with colorectal cancer (8).

To handle genotoxic stress, cells have evolved a number of mechanisms to either repair or tolerate DNA damage (9). In *Saccharomyces cerevisiae*, these pathways include base excision repair (BER) nucleotide excision repair (NER), recombination (REC) and translesion synthesis (TLS) (10). BER primarily involves the repair of base lesions and abasic sites that cause minimal distortion of the DNA helix, and is believed to be the major repair pathway for oxidative DNA damage (11). Ntg1p and Ntg2p are DNA glycosylases with associated AP lyase activity and Apn1p is the major AP endonuclease in yeast (11). It has been shown that *NTG1*, *NTG2* and *APN1* must be eliminated together to severely compromise BER in yeast (12). In contrast to BER, NER is believed to repair bulky, helix-distorting lesions such as bipyrimidine UV photoproducts. Strains (*rad1*) defective in Rad1p, which functions with Rad10p as an endonuclease that cleaves 5′ to the site of damage, are used in this study and have been shown to be completely deficient in NER (11,12). While both BER and NER are DNA repair pathways, owing to their abilities

*To whom correspondence should be addressed. Tel: +1 404 727 0409; Fax: +1 404 727 2618; Email: medpwd@emory.edu

The authors wish it to be known that, in their opinion, the first two authors should be regarded as joint First Authors

to remove and replace DNA damage, recombination and translesion synthesis are known as bypass/tolerance mechanisms since neither may actually remove DNA lesions (13,14). While REC is well known for its role in the repair of DNA single and double-strand breaks, it has also been implicated in the response to oxidative DNA damage and the processing of abasic sites (1,15). Therefore, REC also plays a role in bypass of replication blocking lesions (13). Strains (*rad52*) defective in Rad52p, which help 3′ single-stranded tails invade homolgous duplex DNA, are used in this study and have been shown to be deficient in homologous recombination (11,12). TLS, involving DNA polymerases ζ and η, also functions to bypass DNA replication blocking lesions including oxidative and UV-induced DNA damage (14).

In the present study, we have characterized the cellular effects of increasing H_2O_2 exposures in DNA damage-handling pathway defective strains in order to investigate the relationship between the specific oxidative DNA-damage levels and the ensuing biological consequences resulting from such exposures. WT, BER-defective (*ntg1 ntg2 apn1*), NER-defective (*rad1*), REC-defective (*rad52*), BER/NER-defective (*ntg1 ntg2 apn1 rad1*), BER/REC-defective (*ntg1 ntg2 apn1 rad52*) and NER/REC-defective (*rad1 rad52*) strains were exposed to increasing H_2O_2 doses ranging from low to high toxicity. By quantifying oxidative DNA-damage levels produced by these exposures, we linked specific levels of oxidative DNA damage to H_2O_2-induced responses in transcription, mutation frequency, recombination frequency and intracellular ROS production.

MATERIALS AND METHODS

Strains, media and growth conditions

All strains used in this study are isogenic derivatives of SJR751 (*MATα ade2-101oc his3Δ200 ura3ΔNco lys2ΔBgl leu2-R*). SJR751 will be referred to as wild type (WT). The genotypes of the other strains used in this study are BER-defective strain SJR867 (*MATα ade2-101oc his3Δ200 ura3ΔNco lys2ΔBgl leu2-R ntglΔ::LEU2 ntg2Δ::hisG apn1Δ1::HIS3*), NER-defective strain SJR868 (*MATα ade2-101oc his3Δ200 ura3ΔNco lys2ΔBgl leu2-R rad1Δ::hisG*), REC-defective strain SJR905 (*MATα ade2-101oc his3Δ200 ura3ΔNco lys2ΔBgl leu2-R rad52Δ::URA3*), BER/NER-defective strain SJR1101 (*MATα ade2-101oc his3Δ200 ura3ΔNco lys2ΔBgl leu2-R ntglΔ::LEU2 ntg2Δ::hisG apn1Δ1::HIS3 rad1Δ::hisG*), BER/REC-defective strain SJR908 (*MATα ade2-101oc his3Δ200 ura3ΔNco lys2ΔBgl leu2-R ntglΔ::LEU2 ntg2Δ::hisG apn1Δ1::HIS3 rad52Δ::URA3*), NER/REC-defective strain SJR1134 (*MATα ade2-101oc his3Δ200 ura3ΔNco lys2ΔBgl leu2-R rad1Δ::hisG rad52Δ::URA3*). The genotypes of the strains used for the recombinogenic assays are WT SJR897 (*MATα ade2-101oc his3Δ200 ura3ΔNco-lys2Δ3′-URA3 lys2ΔBgl leu2-R*), BER-defective strain SJR899 (*MATα ade2-101oc his3Δ200 ura3ΔNco lys2Δ3′-URA3 lys2ΔBgl leu2-R ntglΔ::LEU2 ntg2Δ::hisG apn1Δ1::HIS3*), NER-defective strain SJR925 (*MATα ade2-101oc his3Δ200 ura3ΔNco-lys2Δ3′-URA3 lys2ΔBgl leu2-R rad1Δ::hisG*) and BER/NER-defective strain SJR1102 (*MATα ade2-101oc his3Δ200 ura3ΔNco lys2Δ3′-URA3 lys2ΔBgl leu2-R ntglΔ::LEU2 ntg2Δ::hisG apn1Δ1::HIS3 rad1Δ::hisG*). Isogenic strains were constructed as described previously (12). Yeast strains were grown on YPD medium (1% yeast extract, 2% peptone, 2% dextrose and 2% agar for plates). All YPD media were supplemented with adenine sulfate (US Biologicals) at the recommended concentration. For mutagenesis and recombination studies, YNBD media supplemented with required amino acids were utilized (2% glucose, 0.17% yeast nitrogen base without amino acids, 0.5% ammonium sulfate and 2% agar). Supplemented YNBD medium lacking lysine was used for selective growth of Lys^+ recombinants and revertants. Supplemented YNBD medium lacking arginine and containing 60 mg of L-canavanine sulfate (US Biologicals) per liter was used for selective growth of canavanine-resistant (CAN^R) mutants.

DNA isolation and processing

Cell cultures in mid log phase of growth (2×10^7 cell/ml) were harvested, washed once and resuspended to initial volume in water. Cells were treated with 0, 0.5, 5, 25 and 55 mM H_2O_2 for 30 min at 30°C, harvested, and washed twice with water. Alternatively, to determine lesion frequencies under microarray experiment conditions, WT, BER-defective and NER-defective cells were treated in media for 30 min at 30°C with 0.75, 0.4 and 0.3 mM H_2O_2, respectively. Approximately 2×10^9 cells were resuspended in 0.8 ml Sorbitol EDTA (0.9 M sorbitol, 0.1 M EDTA pH 7.4) containing 25 µl DTT (1 M) and 100 µl zymolyase 20T (10 mg/ml) (US Biologicals). Cells were incubated at 37°C overnight. Spheroblasts were spun down, resuspended in 0.5 ml Tris–EDTA (50 ml Tris–HCl pH 7.4, 20 mM EDTA) containing 50 µl of 20 mg/ml proteinase K solution (Qiagen), and incubated at 55°C for 1 h. Then 100 µl of 10% SDS was added and samples were incubated for 20 min at 65°C. After adding 300 µl potassium acetate (5 M), samples were incubated on ice for 30 min. Samples were centrifuged, supernatant transferred and two chloroform extractions were performed. DNA was precipitated with isopropanol, resuspended in TE buffer (10 mM Tris, 1 mM EDTA pH 8.0) and digested with 5 µl ribonuclease A (10 mg/ml) (US Biologicals) at 37°C for 2 h. Samples were precipitated with ethanol, washed twice, lyophilized and resuspended in TE buffer. This DNA extraction procedure was designed to minimize the level of adventitious DNA damage. DNA was quantified by fluorometry using the fluorescent dye bisBENZIMIDE (Hoechst 33258) (Sigma DNA Quantitation Kit, Product No. DNA-QF). Fluorometry was performed according to the manufacturer's recommendations. Yeast DNA aliquots of 10 µg each were digested with BamH1 and ApaL1 (New England BioLabs), using 2.5–3 U of each enzyme per microgram of DNA, for 4 h at 37°C. Digestion with these enzymes yields a 3.7 kb fragment containing the 1.8 kb coding sequence of the *CAN1* gene and 1.9 kb of flanking sequence on chromosome V. After restriction, DNA was precipitated with ethanol, washed twice, lyophilized and resuspended in TE buffer to a concentration of ~1 µg/µl. DNA concentration of the digested samples was determined by the average of at least five independent fluorometric readings.

Alkaline gel electrophoresis

Gel electrophoresis was performed using a 1.1% alkaline agarose gel in alkaline electrophoresis buffer (30 mM NaOH, 2 mM

EDTA pH 8.0) for 20 min at 40 V and then for 15 h at 17 V (16). Genomic DNA samples were prepared as follows. BamH1 and ApaL1 digested genomic DNA of 10 μg was incubated with 5 μg recombinant GST-tagged Ntg1 protein in a 25 μl reaction mixture containing buffer B [15 mM KH_2PO_4, pH 6.8, 10 mM EDTA, 10 mM β-mercaptoethanol and 40 mM KCl (17)]. All sample volumes were equalized by adding TE and then incubated for 30 min at 37°C. To stop the reaction, samples were heated at 60°C for 5 min. An internal standard corresponding to a 710 bp segment of the *CAN1* gene, generated by PCR amplification, was added to each sample after Ntg1p incubation, at a concentration of 0.15 ng per microgram of genomic DNA. Prior to loading, denaturing dye (50 mM NaOH, 1 mM EDTA, pH 8) was added to each sample. The recombinant Ntg1p used in these experiments is N-terminally tagged with glutathione *S*-transferase and expressed in *Escherichia coli* as described previously (17). The protein was purified by glutathione–agarose chromatography followed by Mono-S fast-performance liquid chromatography (18).

Transfer of DNA to membranes and hybridization

Transfer and hybridization were performed as previously described, with the following modifications (19). Transfer was performed utilizing alkaline transfer buffer (20 × SSC, 0.4 M NaOH). After 24 h of transfer, DNA was UV-cross-linked to the nylon membrane and pre-hybridized at 65°C in rapid-hyb buffer (Amersham Biosciences). For hybridization, a 423 bp PCR generated fragment of the *CAN1* gene was the template for a random primed [α-^{32}P]dATP labeled probe. The amount of DNA in the 3.7 kb *CAN1* gene fragment was determined by phosphorimager analysis of the Southern blot. Undamaged DNA (not cleaved by Ntg1p) will yield an intact 3.7 kb band. DNA containing oxidative pyrimidine base damage and abasic sites within this 3.7 kb sequence will be cleaved, resulting in a decrease in the level of the 3.7 kb band (20). All *CAN1* fragment bands were normalized to corresponding internal standard bands to control for sample loading variations. The Poisson expression was used to calculate the number of Ntg1p-recognized lesions per 3.7 kb *CAN1* fragment (21).

Measurement of hydrogen peroxide-induced mutation and recombination frequencies

YPD media was inoculated with a single colony and cells were grown to saturation. With an aliquot of this culture, fresh YPD media was inoculated such that the cell density was 2×10^7 cells/ml after 15 h of growth. Cells were harvested, washed once and resuspended to initial volume in water. Cells were then treated with 0, 0.5, 5, 25 and 55 mM H_2O_2 for 30 min at 30°C, harvested and washed twice with water. To assess Can^R mutations and Lys^+ recombinants, cells were plated as described (12). Both Can^R and Lys^+ colonies were counted three days after selective plating. The mutation and recombination frequencies reported were calculated as the number of mutants or recombinants divided by the total number of colonies. Potential jackpot cultures were identified as outliers statistically by using the Grubbs test (22). These values were withheld from frequency calculations. The data from a minimum of nine independent cultures was used for each mutation and recombination frequency determination.

Microarray analysis of gene expression

Cell cultures were monitored until they reached ~5×10^6 cells/ml and exposed to doses of H_2O_2 that were equitoxic, low doses correspond to 50% survival, while high doses correspond to 1% survival. WT cells were exposed to 0.75 or 5 mM H_2O_2 or left untreated, BER-defective cells were exposed to 0.4 or 5 mM H_2O_2 or left untreated, NER-defective cells were exposed to 0.3 or 3 mM H_2O_2 or left untreated, BER/NER-defective cells were exposed to 0.125 or 0.75 mM H_2O_2 or left untreated for 30 min with shaking at 30°C. Following treatment, cells were harvested and total RNA isolated. Total RNA was extracted from cells using the hot phenol method (23). RNA was then purified on an RNA affinity resin (RNeasy Mini Kit, Qiagen, Chatsworth, CA). The total RNA was ethanol precipitated and resuspended in 15 μl DEPC treated water (RNase free). Total RNA was quantitated by UV spectrophotometry. Approximately 20 μg of total RNA was used in the cDNA synthesis reaction. The cDNA synthesis procedure was carried out as described in the Affymetrix GeneChip Expression Analysis Technical Manual, Chapter 2, Section 4, using a modified oligo(dT) primer with a T7 RNA polymerase promoter on the 5′ end of the sequence [5′-GGCCAGTGAATTGTAATACGACTCACTA-TAGGGAGGCGG-$(dT)_{24}$-3′] and Invitrogen reagents. cDNA was ethanol precipitated and resuspended in 12 μl DEPC water. A 3.3 μl aliquot of cDNA was used for the cRNA biotin labeling reaction. cRNA was labeled with Bio-UTP and Bio-CTP as directed in the ENZO Bioarray High Yield RNA transcript Labeling Kit (ENZO Diagnostics, Farmingdale, NY). cRNA was purified on an affinity resin (RNeasy Mini Kit, Qiagen, Chatsworth, CA). cRNA was fragmented as described in the Affymetrix GeneChip Expression Analysis Technical Manual. Fragmented cRNA was quantitated by measuring absorbance at 260 nm and purity was ascertained by determining the absorbance ratio A_{260nm}/A_{280nm}. All RNA samples yielded ratios of 1.9 or greater indicating good RNA quality.

Chip hybridization and data analysis

The hybridization mix was prepared using ~25 μg of fragmented cRNA and reagents as recommended by the manufacturer to a final volume of 300 μl. The hybridization mix was heated at 99°C for 5 min and then 45°C for 5 min. Following a 5 min centrifugation, 200 μl of the hybridization mixture was loaded onto YSG98 microarray chips (Affymetrix, Santa Clara, CA) containing ~6400 Orfs. Following hybridization, the chips were loaded into the fluidics station for washing and staining as described in Chapter 4, Section 2, of the Affymetrix GeneChip Expression Analysis Technical Manual. After staining and washing, the chips were loaded into the GeneArray Scanner, scanned using a specialized confocal laser scanning microscope, and analyzed using Microarray Suite version 5.0. The arrays were scaled to have a target intensity of 150 in order for all chips to be compared to one another. Integrity of RNA samples was determined by comparing the signal intensity of probes derived from the 5′ and the 3′ ends of both actin and the TATA-binding protein. The signal ratio of 5′ to 3′ did not exceed 2.5-fold, indicating that the mRNA was not degraded during preparation. For all chips, Affymetrix Statistical Algorithms were applied in the analysis of the probe arrays as

described in the Statistical Algorithms Reference Guide (obtainable from Affymetrix, Santa Clara, CA; downloadable at http://www.Affymetrix.com). Changes in expression were determined by comparing global genome expression patterns of cells exposed to H_2O_2 to the corresponding unexposed control. For example, BER/NER-defective cells exposed to 0.125 mM H_2O_2 are compared to BER/NER-defective cells left unexposed. Expression information can be found on our website at (http://www.biochem.emory.edu/labs/medpwd/microarray_index.html). Genes whose expression was up- or down-regulated 2-fold or greater in three replicates for one experiment were included in the hierarchical clustering, which was performed as previously described using the program Cluster and visualized using TreeView (available at http://rana.lbl.gov/EisenSoftware.htm) (24).

Reactive oxygen species levels

ROS were measured with dihydrorhodamine 123 as previously described (25). Mid log phase cell cultures of WT, BER-defective, BER/REC-defective and NER/REC-defective cells were exposed in water to 0, 0.5, 5, 25 or 55 mM H_2O_2 or 0, 0.5, 5, 25 or 55 mM methylmethane sulfonate (MMS) for 30 min at 30°C. These doses of MMS were used because they result in similar toxicities as those reported following H_2O_2 exposure for WT cells. Cell cultures were washed once in water and resuspended in 5 ml of liquid YPD and treated with 25 μg/ml dihydrorhodamine 123 for 2 h at 30°C. Cell cultures were washed and resuspended in phosphate-buffered saline (PBS) and analyzed using a Becton-Dickinson FACSCalibur® and CELLquest® software.

RESULTS

Gene expression patterns of WT and DNA damage-handling defective strains following H_2O_2 exposure

In previous studies, characterization of the yeast global transcriptional response to H_2O_2 has been limited primarily to WT strains. However, recent work has demonstrated that DNA damage-dependent checkpoint activation in G_1 and G_2 phases of the cell cycle does not occur in WT strains exposed to mildly toxic doses of H_2O_2 (26). Activation of these checkpoints in response to mildly toxic doses of H_2O_2 was detected only in BER-compromised strains. Therefore, to identify genes responding specifically to oxidative DNA damage, we evaluated the transcriptional response of not only WT, but also BER-defective, NER-defective and BER/NER-defective cells to moderately and highly toxic doses of H_2O_2, resulting in 50 and 1% survival, respectively. Although the doses of H_2O_2 used are equitoxic among these strains, they are not equimolar (see Materials and Methods). The results shown in Figure 1 represent hierarchical clustering of 1843 genes up- or down-regulated 2-fold or greater, for a particular strain and H_2O_2 dose, in three independent experiments. Genes are represented as red, green or black, indicating up-regulation, down-regulation, or no change, respectively. The experiments cluster according to their overall expression patterns. The clustering of experiments was divided into Groups I–IV (Figure 1). The complete microarray data set is available at (http://www.biochem.emory.edu/labs/medpwd/microarray_index.html) and reports the specific transcriptional changes for individual genes.

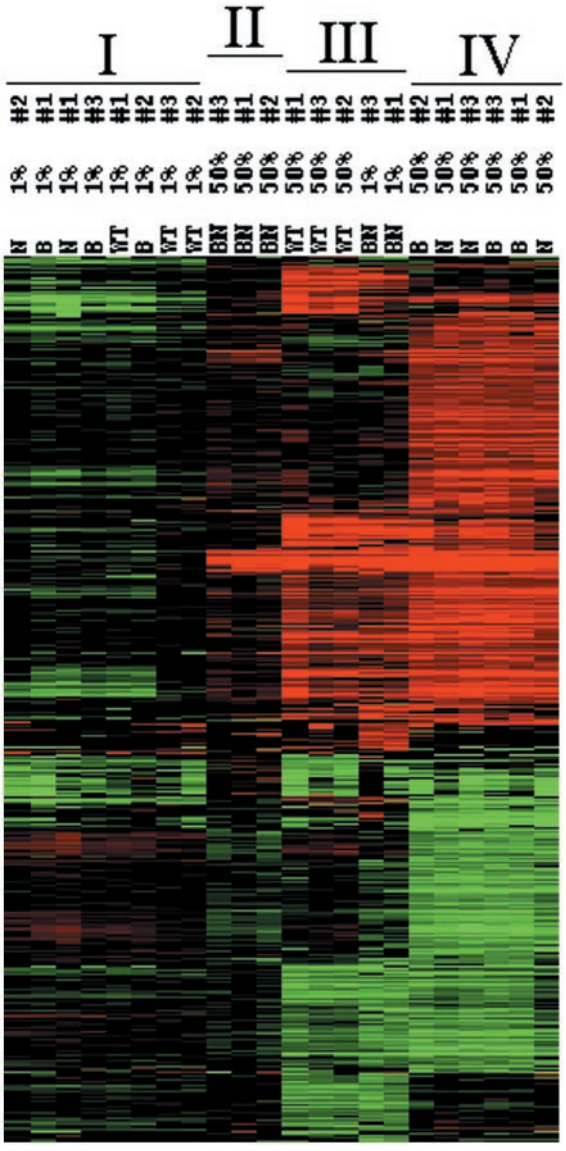

Figure 1. Hierarchical clustering of H_2O_2-induced transcriptional changes in DNA damage-handling pathway defective strains. 1843 genes up- or down-regulated 2-fold or greater are represented. Genes are represented horizontally for each experiment and designated as red, green or black, indicating up-regulation, down-regulation or no change, respectively. Clustering of experiments was divided into Groups I–IV according to overall expression patterns. WT, wild type; B, BER-defective; N, NER-defective; BN, BER/NER-defective. Percentages indicate percentage survival following H_2O_2 treatment, and the numbers represent experiment number.

Group I includes WT, BER-defective and NER-defective cells exposed to highly toxic doses (5, 5, and 3 mM, respectively) of H_2O_2 (Figure 1). The expression patterns of these cells reveal a global down-regulation of genes. Highly toxic H_2O_2 exposures have been demonstrated to induce apoptotic-like phenotypes such as chromatin alterations (27,28). Since these chromatin alterations might prevent proper transcription, we probed WT cells, following exposures to highly toxic doses of H_2O_2, for apoptotic indicators such as caspase activation, annexin V and TUNEL positive staining (25,29).

No apoptotic-like phenotypes were observed following H_2O_2 exposures identical to exposures employed for the microarray analysis (data not shown). However, apoptotic-like phenotypes were observed using higher (20-fold) doses and longer (3 h) exposure times (data not shown). Alternatively, because H_2O_2 exposure causes base damage, single-strand breaks and abasic sites, which arrest RNA polymerase II, these results may reflect transcriptional arrest in response to DNA damage (30). If RNA polymerase is blocked by DNA damage occurring extensively across the genome, transcription will be globally decreased.

Group II represents BER/NER-defective cells exposed to a moderately toxic (50% survival) dose of H_2O_2 (0.125 mM) (Figure 1). Fifty one genes were up-regulated and one gene was down-regulated. Genes identified in this group are either unknown in function or involved mainly in cell stress and mitochondrial maintenance such as *TSA2*, *CTA1*, *TRR1*, *GTT2*, *SOD2*, *CCP1*, *CYC1*. We have shown previously that DNA damage signaling occurs in BER/NER-defective cells in response to unrepaired, spontaneous oxidative DNA damage (31). Accordingly, our results suggest that in BER/NER-defective cells in which a spontaneous DNA damage response has already been elicited, no additional DNA damage response is produced following subsequent H_2O_2 exposure.

Similarly, Group III represented by WT and BER/NER-defective cells exposed to 0.75 mM H_2O_2, also revealed genes involved in the general stress response to H_2O_2 (Figure 1). Many genes observed in other studies (32,33) as up- or down-regulated in response to H_2O_2 exhibited similar transcriptional changes in our experiments. For example, increased expression of specific transcriptional regulators of the oxidative stress response including, *ROX1*, *HAP2* and *HAP4* was observed. Up-regulation of genes involved in cell stress, mitochondrial maintenance, carbohydrate metabolism, degradation and other functional categories were also observed. Genes encoding transport, ribosomal proteins, translational factors and cell-cycle-initiation factors, which have been observed in other studies to be down-regulated by H_2O_2, were also down-regulated in our experiments (32,33). In addition, because 0.75 mM H_2O_2 resulted in 50 and 1% survival in the WT and BER/NER-defective strains, respectively, these results reveal that it is the H_2O_2 exposure dose and not the level of toxicity attached with that dose (as measured by survival) that determines the transcriptional response.

Group IV represents BER-defective and NER-defective cells exposed to moderately toxic doses of H_2O_2 (0.3 and 0.4 mM, respectively) (Figure 1). While the genes that are up- and down-regulated in these cells include known responders to oxidative stress, many of which are also observed in Group III, a subset of genes identified as specific to Group IV are designated as candidates responding specifically to induced, oxidative DNA damage (Table 1). This is supported by the inclusion of a number of genes known to be involved in DNA repair that are specific to Group IV, but are not up-regulated in WT cells in response to a moderately toxic dose of H_2O_2. Table 1 lists the candidate genes that are thought to be responding specifically to induced, oxidative DNA damage. These genes are arranged by functional category such as DNA repair/metabolism, cell stress, transcription and signal transduction. The compilation of all functional

Table 1. Candidate genes responding to induced, oxidative DNA damage

Gene name	BER-defective[a]	NER-defective[a]	Gene description[c]
DNA repair/Metabolism			
RAD4	2.8	2.9	Nucleotide excision repair protein
RAD2	NC[b]	2.7	Nucleotide excision repair protein
RAD28	2.5	2.7	Protein involved in the same pathway as Rad26p, involved in transcription coupled repair
MAG1	2.1	2.1	3-Methyladenine DNA glycosylase
PHR1	3.8	3.6	Photolyase
MHR1	2.4	2.5	Involved in mitochondrial homologous DNA recombination
HSM3	2.5	NC	Putative member of the yeast MutS homolog family
DUN1	2.1	NC	Protein kinase involved in DNA damage response
SRL3	NC	3.0	Suppressor of RAD53 lethality, nucleotide metabolism
RNR3	NC	5.9	Ribonucleotide reductase large subunit
MMS2	NC	2.0	Ubiquitin conjugating enzyme, member of error-free post-replication DNA repair pathway
DDR48	NC	2.3	DNA-damage responsive protein
DDI1	NC	2.8	DNA damage inducible
Cell stress			
ZTA1	4.7	5.1	Homolog to quinine oxidoreductase (*E.coli*)
TRR2	2.7	2.8	Thioredoxin reductase
TTR1	NC	2.3	Glutaredoxin (thioltransferase)
TRX3	NC	2.5	Thioredoxin type II
GLR1	NC	2.5	Glutathione oxidoreductase
POS5	2.5	2.3	Involved in oxidative stress
YBR070C	2.2	NC	Expression is regulated by stress conditions
ROD1	3.4	NC	Involved in drug resistance
Signal transduction			
YPK1	NC	2.1	Serine/threonine protein kinase
IKS1	6.0	5.5	Probable serine/threonine protein kinase
BCY1	NC	2.3	Regulatory subunit of cAMP-dependent protein kinase
CMK1	3.3	3.4	Calmodulin-dependent protein kinase
RIM15	2.2	2.4	Protein kinase involved in meiosis
PKH1	NC	2.4	Serine/threonine protein kinase
PPM1	3.1	3.7	Carboxy methyl transferase for protein phosphatase 2A catalytic subunit
PPZ2	3.0	3.8	Serine/threonine phosphatase Z
KIN1	2.4	2.4	Serine/threonine protein kinase
PPH21	2.5	2.2	Serine/threonine protein phosphatase 2A
PTP1	2.5	2.5	Phosphotyrosine-specific protein phosphatase
GIP1	28.5	19.1	Protein phosphatase 1
PTC3	2.5	2.4	Protein phosphatase type 2C
SMK1	25.8	17.9	MAP kinase
RRD2	NC	4.8	Protein phosphatase type 2A
PKH2	4.3	3.9	Serine/threonine protein kinase
GLC8	3.8	2.7	Regulates activity of protein phosphatase 1
RIM11	2.5	2.9	Serine/threonine protein kinase
CMP2	3.1	2.5	Catalytic A subunit of calcineurin

Table 1. *Continued*

GPA2	2.2	NC	Potential role in regulation of cAMP levels
KIN82	3.1	NC	Putative serine/threonine protein kinase
BRO1	2.8	NC	Involved in resistance to osmotic shock
STE11	2.5	NC	MEKK homolog, serine/threonine protein kinase
Transcription			
CAF17	5.2	5.3	CCR4 associated factor
OAF1	NC	2.6	Peroxisome proliferating transcription factor
YAP5	2.0	2.5	bZIP protein, transcription factor
YAP1	4.3	3.5	Jun-like transcription factor
IMP2	3.3	3.0	Transcription factor
TFG2	2.8	2.4	Transcription initiation factor TFIIF middle subunit
GTS1	5.0	4.6	Specific RNA polymerase II transcription factor
SIP2	2.7	2.9	Interacts with Snf1p and Snf4p
NPR2	NC	2.7	Putative post-transcriptional regulator
CAD1	4.2	3.5	Transcriptional activator
PHO2	3.3	3.1	Positive regulator of PHO5 and other genes
PHO85	NC	2.3	Negative transcriptional regulator
HAP5	2.4	2.8	Component of CCAAT-binding transcription factor
YRR1	3.6	3.9	Transcription factor
MET28	4.7	NC	Transcriptional activator
CST6	2.6	2.3	Chromosome stability
SPT3	2.2	NC	Transcription factor, member of SAGA complex
MED2	2.3	NC	RNA polymerase II transcriptional regulation mediator
UGA3	2.4	NC	Zinc-finger transcription factor
TFC7	2.5	NC	TFIIC (transcription initiation factor) subunit
CST9	NC	3.1	Similarity to chicken RING zinc finger protein

[a]Average fold change (represents average of three independent experiments) for experiments where cells are exposed to a dose of H_2O_2 resulting in 50% survival (0.4 mM for BER-defective cells and 0.3 mM for NER-defective cells).
[b]NC means no change between experimental and control samples.
[c]Obtained from the *Saccharomyces cerevisiae* database http://www.yeastgenome.org/.

groups observed in this study can be found at (http://www.biochem.emory.edu/labs/medpwd/microarray_index.html).

To address the notion that transcriptional changes due specifically to H_2O_2-induced DNA damage occur in BER-defective and NER-defective cells but not WT cells under our conditions, oxidative DNA damage levels were determined using a gene-specific DNA damage-detection assay. WT, BER-defective and NER-defective strains were exposed to 0.75, 0.4 and 0.3 mM H_2O_2, respectively. These doses are identical to those used for the microarray experiments that resulted in 50% survival (see Materials and Methods). Following H_2O_2 exposure during log phase of growth, DNA was extracted, restricted and treated with Ntg1p from *S.cerevisiae*, an *N*-glycosylase with associated AP-lyase activity, that primarily recognizes and cleaves DNA containing oxidized pyrimidines and abasic sites (17). Southern blot analysis was used to determine DNA damage levels for a 3.7 kb DNA fragment containing the *CAN1* gene (20). Using the ratio of band intensities of Ntg1p treated to untreated samples, the Poisson formula was used to calculate the frequency of Ntg1p-recognized DNA lesions per 3.7 kb fragment (21). This value was used to extrapolate the frequency of lesions per genome.

Following H_2O_2 exposure of the WT strain, the *CAN1* band intensity of Ntg1p-treated and untreated DNA samples was equivalent (1.04 ± 0.12, ratio of band intensity). Therefore, no detectable level of DNA damage was observed in the WT strain. However, the NER-defective and BER-defective strains displayed elevated levels of oxidative DNA damage, 520 (0.85 ± 0.073, ratio of band intensity) and 940 (0.75 ± 0.056, ratio of band intensity) Ntg1p-recognized lesions per genome, respectively. The elevated level of Ntg1p-recognized lesions following H_2O_2 exposure in NER-defective cells is likely due to the presence of unrepaired Ntg1p-recognized lesions such as abasic sites that can also repaired by NER (12,34–36). These data indicate that candidate transcriptional responders to exogenously induced, oxidative DNA damage may be revealed from the BER-defective and NER-defective strain gene expression profiles.

Preference for REC versus TLS in handling H_2O_2-induced DNA damage

To gain insight into the potential interrelationships among the DNA damage-handling pathways in their responses to exogenous oxidative stress, mutation and recombination frequency analyses of strains defective in BER, NER, REC, BER/NER, BER/REC and NER/REC were performed. Mutation frequency was monitored using the *CAN1* locus. Forward mutations in the *CAN1* gene render the locus non-functional and the cells resistant to L-canavanine (37). For recombination measurements, recombination between two non-functional *LYS2* alleles was measured by Lys^+ prototroph production (38).

The spontaneous mutation frequencies of the NER-defective, REC-defective and BER-defective strains were elevated 3.3-, 15-, and 21-fold, respectively, above that of WT (Figure 2A). Following increasing exposures to H_2O_2, a maximum mutation frequency of approximately 1.1×10^{-4} was induced in these strains as well as WT. While the WT, NER-defective and REC-defective strains reached this frequency following 55 mM H_2O_2 exposure, the BER-defective strain reached this frequency at a much lower H_2O_2 exposure (5 mM) and did not increase further following exposures to higher doses of H_2O_2 (Figure 2A). The recombination frequency of the BER-defective strain, however, increased with H_2O_2 exposure doses (Figure 2C). Since recombination frequency, but not mutation frequency increased in response to a range (5–55 mM) of H_2O_2 exposures, these results suggest a preference for using REC versus error-prone TLS in processing H_2O_2-induced DNA lesions when BER is compromised.

As indicated above, the WT and single pathway defective strains displayed a maximum mutation frequency following exposures to increasing doses of H_2O_2 (Figure 2A). This maximum mutation frequency level may represent saturation of the

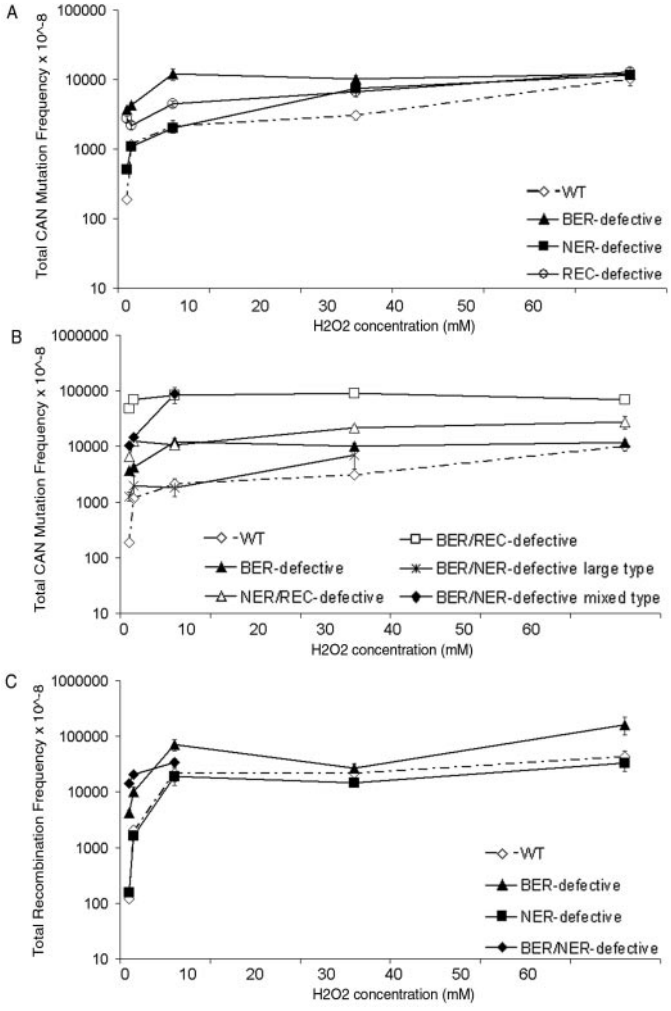

Figure 2. H_2O_2-induced genetic instability phenotypes of DNA damage-handling pathway defective strains. (**A** and **B**) Total CAN^R mutation frequencies of WT (open diamond), BER-defective (closed triangle), NER-defective (closed square), REC-defective (open circle), BER/REC-defective (open square), NER/REC-defective (open triangle), BER/NER-defective large cell type (asterisk) and BER/NER-defective mixed cell type (closed diamond). (**C**) Total recombination frequencies of WT (open diamond), BER-defective (closed triangle), NER-defective (closed square), and BER/NER-defective cells (closed diamond). Results represent the average of a minimum of nine independent experiments. Error bars represent the standard error of the mean.

DNA damage-handling capacity of the TLS pathway. To test whether the TLS pathway is capable of handling additional DNA damage, we determined H_2O_2-induced mutation frequencies in double pathway defective strains (Figure 2B). In response to 0.5 mM H_2O_2, the NER/REC-defective strain produced the maximum mutation frequency of the WT and single pathway defective strains. However, at H_2O_2 exposures above 5 mM, mutation frequency continued to increase. This suggests that, under these conditions, the TLS pathway in the surviving cell population is not saturated in its DNA damage-handling ability. These results also suggest that in NER/REC-defective cells, with the BER and TLS pathways remaining, the maximum level of DNA damage capable of being processed by the BER pathway may be exceeded at H_2O_2 exposures >5 mM. Therefore, any additional DNA damage must be handled by the TLS pathway.

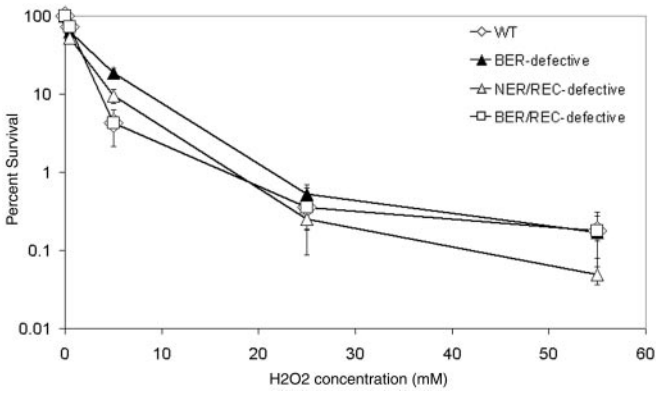

Figure 3. Sensitivity of DNA damage-handling pathway defective strains to H_2O_2. WT (open diamond), BER-defective (closed triangle), BER/REC-defective (open square) and NER/REC-defective (open triangle) cells were exposed to 0, 0.5, 5, 25 and 55 mM H_2O_2. Results represent the average of a minimum of nine independent experiments. Error bars represent the standard error of the mean.

In contrast to the NER/REC-defective strain, the BER/REC-defective strain produced a spontaneous mutation frequency substantially elevated above the spontaneous and induced frequencies of all other strains (Figure 2B). Exposure of the BER/REC-defective strain to increasing doses of H_2O_2 failed to further increase mutation frequency. These results underscore the importance of BER and REC in the processing of oxidative DNA damage. In addition, these findings also indicate that in the absence of both BER and REC, the TLS pathway may be saturated with respect to its DNA damage-handling ability. Only the BER/NER-defective strain, when exposed to 5 mM H_2O_2, reached comparable mutation frequency levels observed with the BER/REC-defective strain (Figure 2B). However, exposure of the BER/NER-defective strain to H_2O_2 doses > 5 mM caused extensive cytotoxicity (>99.8%, data not shown). These results suggest that in the absence of BER, NER is required to process a subset of cytotoxic lesions that are not handled by REC.

Levels of H_2O_2-induced DNA damage differ among DNA damage-handling pathway defective strains

To establish a relationship between specific levels of H_2O_2-induced DNA damage and resulting biological consequences, the *CAN1* gene-specific DNA damage-detection assay was utilized. WT, BER-defective, BER/REC-defective and NER/REC-defective cells were exposed to doses of H_2O_2 resulting in low to high toxicity (Figure 3). These strains were chosen due to their mutation and recombination frequency phenotypes. For example, the BER/REC-defective strain did not exhibit a dose-dependent increase in mutation frequency; therefore, it was necessary to determine whether increasing H_2O_2 exposures also resulted in increases in DNA damage levels. DNA damage levels were not determined for the BER/NER-defective strain due to its extreme sensitivity to low doses of H_2O_2.

A dose-dependent increase in Ntg1p-recognized DNA lesions was observed in WT and BER-defective cells with increasing exposures to H_2O_2 (Table 2). However, for each H_2O_2 exposure, the amount of DNA damage detected in the

Table 2. Ntg1p-recognized DNA lesions in the *CAN1* locus[a] and the overall genome[b]

[H_2O_2]	0 mM	0.5 mM	5 mM	25 mM	55 mM
WT	0 (1.0 ± 0.030)	210 (0.94 ± 0.090)	1270 (0.68 ± 0.060)	2240 (0.50 ± 0.046)	3890 (0.31 ± 0.039)
BER-defective	390 (0.89 ± 0.061)	1200 (0.69 ± 0.077)	2820 (0.42 ± 0.022)	3570 (0.33 ± 0.042)	4870 (0.23 ± 0.040)
BER/REC-defective	970 (0.74 ± 0.065)	1200 (0.69 ± 0.057)	2470 (0.47 ± 0.044)	2110 (0.52 ± 0.036)	2600 (0.45 ± 0.059)
NER/REC-defective	940 (0.75 ± 0.063)	970 (0.74 ± 0.070)	940 (0.75 ± 0.036)	1400 (0.71 ± 0.048)	3240 (0.39 ± 0.028)

[a]Values in parentheses represent the ratio of band intensities of Ntg1p treated to untreated samples ± the standard error of the mean.
[b]Values were extrapolated from calculation of lesions per 3.7 kb *CAN1* fragment as described in the text and represent approximate number of lesions per genome.

BER-defective strain was significantly elevated above that of the WT strain. Unexpectedly, in the BER/REC-defective and NER/REC defective strains, Ntg1p-recognized lesions did not increase in a dose-dependent manner with increasing doses of H_2O_2. The BER/REC-defective strain exhibited an increase in Ntg1p-recognized lesions between H_2O_2 exposures of 0.5 and 5 mM, but did not increase further with H_2O_2 exposures >5 mM. In the NER/REC-defective strain, no increase in Ntg1p-recognized lesions was observed until cells were exposed to H_2O_2 doses > 5 mM. These results suggest that in WT and NER/REC-defective cells, at H_2O_2 exposures of <5 mM, efficient handling of DNA damage by the BER pathway prevents an increase in Ntg1p-recognized lesions. However, the increase in DNA damage levels induced by H_2O_2 doses >5 mM suggests that in the NER/REC-defective strain, the DNA damage-handling capacity of the BER pathway may be exceeded.

Unrepaired DNA damage alone causes increases in intracellular ROS

The unexpected H_2O_2-induced lesion frequencies determined for the BER/REC-defective and NER/REC-defective strains may be indicative of a diverse, heterogeneous population of cells that have mixed responses to H_2O_2 exposures within that population. Therefore, we determined intracellular ROS levels of WT, BER-defective, BER/REC-defective and NER/REC-defective strains, following exposures to increasing doses of H_2O_2 (Figure 4A and B). A dose-dependent increase in intracellular ROS levels was observed in the WT, BER-defective, BER/REC-defective and NER/REC-defective cells (Figure 4A). However, the level of intracellular ROS produced in response to a particular dose of H_2O_2 varied between the strains. For example, the levels of intracellular ROS generated by 5, 25 and 55 mM H_2O_2 exposures were elevated in BER-defective, BER/REC-defective and NER/REC-defective cells relative to WT (Figure 4B). Yet, unlike the BER-defective strain, for which, at 25 and 55 mM, a single, pronounced ROS peak was observed, two ROS peaks were observed in the BER/REC-defective and NER/REC-defective strains at these same doses (Figure 4A). The presence of these two peaks suggests that these strains are composed of a population of cells exhibiting mixed responses to H_2O_2 exposure.

The elevated intracellular ROS levels in the DNA damage-handling pathway defective strains exposed to the same doses of H_2O_2, relative to WT, suggest that unrepaired DNA damage causes increases in intracellular ROS levels. This idea is supported by our observations that both DNA damage and intracellular ROS levels are elevated under normal growth conditions (i.e. no exogenous H_2O_2 exposure) in BER/NER-defective, BER/REC-defective and NER/REC-defective cells [(31) and Figure 2B]. The increase in intracellular ROS in the BER/REC-defective and NER/REC-defective cells under normal growth conditions is evidenced by the slight shift of the peaks to the right relative to WT (Figure 2B). To further address whether unrepaired DNA damage alone causes an increase in intracellular ROS, WT, BER-defective, BER/REC-defective and NER/REC-defective strains were exposed to methylmethane sulfonate (MMS), a DNA alkylating agent. Unlike H_2O_2, MMS is not converted into ROS and does not cause oxidative DNA damage. Thus, exposure to MMS would not be expected to directly cause increases in intracellular ROS (9). However, similar to H_2O_2, MMS induced a dose-dependent increase in intracellular ROS levels in all four strains (Figure 5A). In addition, the BER/REC-defective, and NER/REC-defective cells produced higher levels of intracellular ROS in response to the same dose of MMS compared to WT cells (Figure 5B). These data indicate that the greatest increases in intracellular ROS caused by MMS-induced DNA damage occur in those strains (BER/REC-defective and NER/REC-defective) with multiple DNA damage-handling pathway defects. These results also support the notion that DNA damage alone causes increases in intracellular ROS in yeast.

DISCUSSION

Reactive oxygen species are generated by aerobic metabolism and exposure to exogenous agents, such as H_2O_2 (3). Therefore, cellular exposure to ROS is unavoidable. While ROS mediate a necessary and vital role in signal transduction, the consequences of ROS exposure are generally regarded to be adverse (39). For example, ROS can damage various cellular components, including DNA (1,2). To handle oxidative DNA damage, cells have evolved a number of DNA repair and damage tolerance mechanisms (1,10). In yeast, these mechanisms include the BER, NER, REC and TLS pathways. In this study, we have characterized the response of yeast cells, defective in one or two of these DNA damage-handling pathways, to exogenous oxidative stress. Our results allow establishment of a relationship between specific DNA damage levels induced by H_2O_2 and the corresponding biological responses. ROS and the DNA damage it produces are implicated in the etiology of degenerative cellular conditions such as, cancer, neurodegenerative and cardiovascular disease, and age-related pathological changes (2,3,5). Because DNA damage-handling mechanisms are highly conserved between yeast and humans, our work may reveal new insights into the etiology of these human disease states as they relate to the roles of ROS.

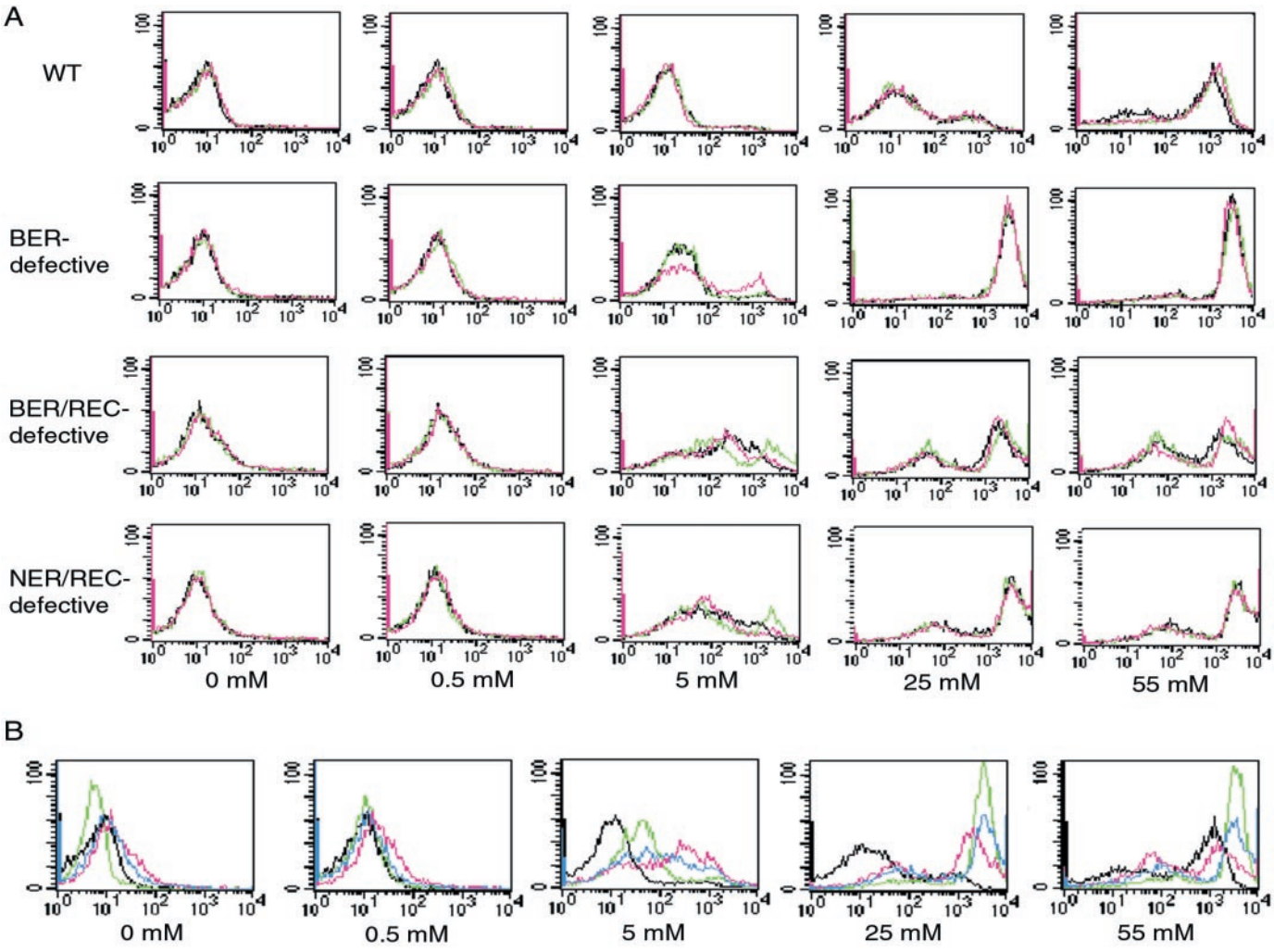

Figure 4. Flow cytometric analysis of H_2O_2-induced ROS levels in DNA damage-handling pathway defective strains. (**A**) FACS profiles of WT, BER-defective, BER/REC-defective and NER/REC-defective cells exposed to 0, 0.5, 5, 25 and 55 mM H_2O_2. Three independent experiments (black, pink and green lines) are represented on each profile. (**B**) Comparison of intracellular ROS levels between WT (black), BER-defective (green), BER/NER-defective (pink) and NER/REC-defective (blue) cells for each H_2O_2 concentration represented in (A). Results from a single representative experiment are shown. X-axis, from left to right, represents increasing levels of intracellular ROS as determined by dihydrorhodamine fluorescence.

Previous work by our group has demonstrated that in BER/NER-defective cells under normal growth conditions, accumulated DNA damage levels in the range of 1400 Ntg1p-recognized lesions per genome result in profound changes in gene expression (31). In the present study, we demonstrate that exogenous exposure of BER/NER-defective cells to H_2O_2 does not result in significant transcriptional changes in response to induced, oxidative DNA damage. These results suggest that when a DNA damage response has been elicited by specific levels of unrepaired, spontaneous DNA damage, no additional DNA damage response is induced by subsequent exogenous H_2O_2 exposure.

Our gene expression analysis also identified genes responding specifically to induced, oxidative DNA damage. We show that under conditions of H_2O_2 exposure identical to those used for the microarray experiments, the BER-defective and NER-defective strains contain significant levels of unrepaired, oxidative DNA damage. This situation is in contrast to the WT strain, which did not contain significant levels of oxidative DNA damage and did not show these transcriptional response patterns. These results support the notion that under such H_2O_2 exposure conditions, candidate genes responding to induced oxidative stress may be identified in the BER-defective and NER-defective strains, but not the WT strain. In addition, we identified genes induced by oxidative stress in our study that were also identified by Samson and colleagues as sensitive to oxidative stress when deleted (see http://genomicphenotyping.mit.edu). Significantly, there was greater correspondence of genes identified in both our study and that of Samson and colleagues in the repair defective strains compared to WT. These findings further validate our approach for the identification of genes responding specifically to the presence of oxidative DNA damage induced by ROS.

By exposing our yeast strains to doses of H_2O_2 ranging from low to high toxicity, we demonstrated the capacities of and preferences for particular DNA damage-handling pathways in the processing of oxidative DNA damage. In the absence of BER, REC appears to have a higher capacity than NER for handling spontaneous, oxidative DNA damage. In addition, in the absence of BER, REC was preferred over the error-prone

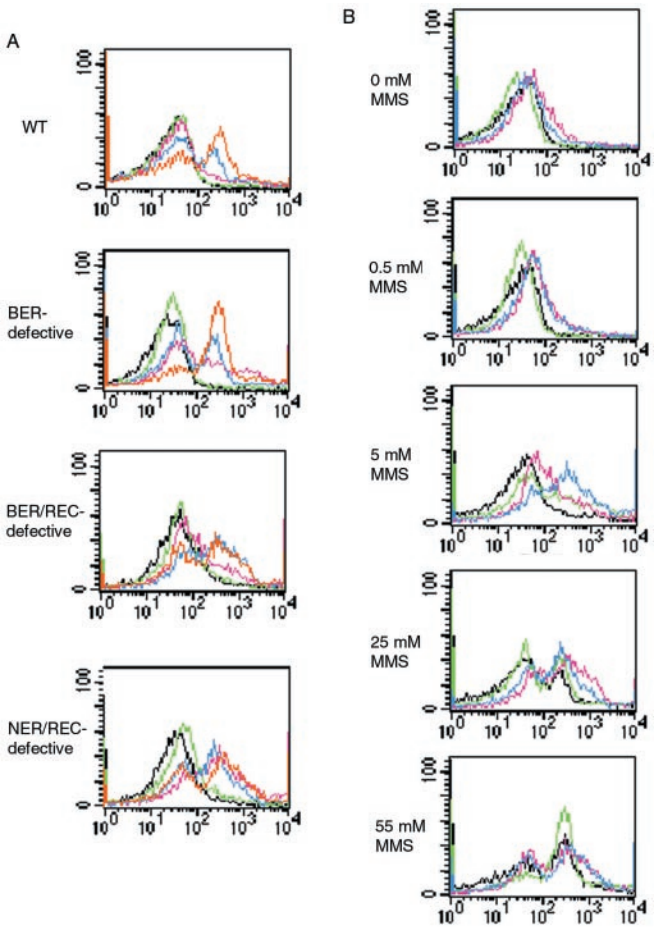

Figure 5. Flow cytometric analysis of MMS-induced ROS levels in DNA damage-handling pathway defective strains. (**A**) FACS profile of WT, BER-defective, BER/REC-defective and NER/REC-defective cells exposed to 0 mM (black), 0.5 mM (green), 5 mM (pink), 25 mM (blue) and 55 mM (orange) MMS. (**B**) Comparison of intracellular ROS levels between WT (black), BER-defective (green), BER/REC-defective (blue) and NER/REC-defective (pink). X-axis, from left to right, represents increasing levels of intracellular ROS.

TLS pathway in handling induced, oxidative DNA damage as demonstrated by the increase in recombination frequency but not mutation frequency following increasing H_2O_2 exposures (Figure 2). Furthermore, we observed that while the BER/REC-defective strain is viable, but genetically unstable following H_2O_2 exposure, the BER/NER-defective strain is exquisitely sensitive to the toxic effects of equivalent doses. Therefore, while REC is preferred over NER for handling spontaneous and induced oxidative DNA lesions, in the absence of BER, the NER pathway is necessary for repair of a subset of cytotoxic DNA lesions. One example may be the bulky, oxidative DNA lesion, 8, 5′-(*S*)-cyclo-2′-deoxyadenosine that is known to be repaired by NER, but not BER (40).

Determination of the levels of induced, oxidative DNA damage revealed that, unlike the WT and BER-defective strains, the BER/REC-defective and NER/REC-defective strains did not display a dose-dependent increase in induced, oxidative DNA damage levels in response to increasing H_2O_2 exposures. Following exposures to high (55 mM) H_2O_2 doses, the DNA damage levels detected for the NER/REC-defective and BER/REC-defective strains were significantly lower than those of the WT and BER-defective strains. The NER/REC-defective and BER/REC-defective strains appear to resist introduction of additional oxidative DNA damage from exogenous ROS better than the WT or BER-defective strains. This may be due to the induction of a stress response state by unrepaired, spontaneously-induced DNA damage in the NER/REC-defective and BER/REC-defective cells. We have previously demonstrated that elevated levels of unrepaired, spontaneous DNA damage in BER/NER-defective cells cause profound changes in gene expression (31). Transcriptional changes may also occur in NER/REC-defective and BER/REC-defective cells since these strains contain spontaneous DNA damage levels comparable to the BER/NER-defective strain, approximately 1000 (BER/REC-defective and NER/REC-defective cells) versus 1400 (BER/NER-defective cells) Ntg1p-recognized lesions per genome. These transcriptional changes may include a number of genes known to be involved in DNA damage that are also induced by DNA damage such as *NTG1*, as well as other genes that are up-regulated in BER/NER-defective cells under normal growth conditions (31,41).

The NER/REC-defective and BER/REC-defective strains contain a sub-population of cells that produce less intracellular ROS than WT and BER-defective strains in response to identical H_2O_2 exposures (Figure 4). These data support the notion that strains containing elevated levels of spontaneous DNA damage exhibit different abilities in handling additional oxidative stress from exogenous sources. However, in general, we observed that strains compromised in DNA repair produce higher levels of ROS per equivalent H_2O_2 exposure compared to WT. This suggests that DNA damage alone causes an increase in intracellular ROS, and is further supported by the observed increases in intracellular ROS following MMS exposure (Figure 5). BER/NER-defective, BER/REC-defective and NER/REC-defective strains, which differ from the WT strain only in their ability to repair/handle spontaneous DNA damage, display elevated levels of unrepaired DNA damage commensurate with elevated levels of intracellular ROS. Therefore, we conclude that DNA damage alone causes an increase in intracellular ROS in yeast. ROS are generated through a variety of metabolic pathways including the NADPH oxidase systems, and are important for signal transduction pathways involved in the control of transcription and cell growth (3,4,39). However, it is not clear how ROS function in such signal transduction pathways. Our results suggest that ROS may function in signal transduction pathways mediating the response to unrepaired DNA damage. In addition, ROS may also function in post-translational modifications of proteins involved in DNA repair. For example, *Rnr*3p, a known DNA repair protein, is regulated by its redox state (42).

Given the conservation of the DNA damage-handling pathways between yeast and humans, our results in yeast may provide insights into the roles of DNA damage and ROS in degenerative cellular conditions in higher eukaryotes. In mammalian cells, elevated levels of ROS have been linked to several aspects of carcinogenesis (43). For example, ROS causes DNA damage, which in turn contributes to genetic instability (8). In addition, since ROS are involved in signal transduction pathways, an abundance of ROS may trigger continuous activation of oncogenes and transcription factors

(44). Such events, as well as ROS damage to proteins may contribute to tumor progression by promoting metastasis and invasion of tumor cells to surrounding tissues (43,44). Elevated levels of ROS cause induction of antioxidant defense systems, which could contribute to tumor cell resistance to certain chemotherapeutic agents (43,44). Accordingly, we demonstrate that cells possessing elevated levels of unrepaired, spontaneous DNA damage also have increased levels of intracellular ROS and exhibit altered abilities to resist additional, exogenous oxidative stress (Figure 4 and Table 2).

While the role of unrepaired DNA damage in mutagenesis and the initiation of carcinogenesis in mammalian cells is well established, its contribution to tumor promotion and progression is less well understood. Our results linking DNA damage and intracellular ROS production may provide insights into the contribution of DNA damage to tumor promotion and progression. Following accumulation of specific levels of unrepaired DNA damage, the subsequent increases in intracellular ROS levels may facilitate tumor promotion and progression by increasing genetic instability, activating oncogenes and contributing to resistance to chemotherapeutic agents (43,44).

ACKNOWLEDGEMENTS

We are grateful for comments and suggestions from Drs Wolfram Siede, Tina Saxowsky and Natalya Degtyareva. This work was supported by NIH grant ES11163.

REFERENCES

1. Slupphaug,G., Kavli,B. and Krokan,H.E. (2003) The interacting pathways for prevention and repair of oxidative DNA damage. *Mutat. Res.*, **531**, 231–251.
2. Cooke,M.S., Evans,M.D., Dizdaroglu,M. and Lunec,J. (2003) Oxidative DNA damage: mechanisms, mutation, and disease. *FASEB J.*, **17**, 1195–1214.
3. Finkel,T. and Holbrook,N.J. (2000) Oxidants, oxidative stress and the biology of ageing. *Nature*, **408**, 239–247.
4. Costa,V. and Moradas-Ferreira,P. (2001) Oxidative stress and signal transduction in *Saccharomyces cerevisiae*: insights into ageing, apoptosis and diseases. *Mol. Aspects Med.*, **22**, 217–246.
5. Szatrowski,T.P. and Nathan,C.F. (1991) Production of large amounts of hydrogen peroxide by human tumor cells. *Cancer Res.*, **51**, 794–798.
6. Malins,D.C., Polissar,N.L. and Gunselman,S.J. (1996) Progression of human breast cancers to the metastatic state is linked to hydroxyl radical-induced DNA damage. *Proc. Natl Acad. Sci. USA*, **93**, 2557–2563.
7. Girard,P.M. and Boiteux,S. (1997) Repair of oxidized DNA bases in the yeast *Saccharomyces cerevisiae*. *Biochimie*, **79**, 559–566.
8. Jackson,A.L., Chen,R. and Loeb,L.A. (1998) Induction of microsatellite instability by oxidative DNA damage. *Proc. Natl Acad. Sci. USA*, **95**, 12468–12473.
9. Friedberg,E.C., Walker,G. and Siede,W. (1995) *DNA Repair and Mutagenesis*. ASM Press, Washington, DC.
10. Doetsch,P.W., Morey,N.J., Swanson,R.L. and Jinks-Robertson,S. (2001) Yeast base excision repair: interconnections and networks. *Prog. Nucleic Acids Res. Mol. Biol.*, **68**, 29–39.
11. Lindahl,T. and Wood,R.D. (1999) Quality control by DNA repair. *Science*, **286**, 1897–1905.
12. Swanson,R.L., Morey,N.J., Doetsch,P.W. and Jinks-Robertson,S. (1999) Overlapping specificities of base excision repair, nucleotide excision repair, recombination, and translesion synthesis pathways for DNA base damage in *Saccharomyces cerevisiae*. *Mol. Cell. Biol.*, **19**, 2929–2935.
13. Cox,M.M. (2002) The nonmutagenic repair of broken replication forks via recombination. *Mutat. Res.*, **510**, 107–120.
14. Hoeijmakers,J.H. (2001) Genome maintenance mechanisms for preventing cancer. *Nature*, **411**, 366–374.
15. Otterlei,M., Kavli,B., Standal,R., Skjelbred,C., Bharati,S. and Krokan,H.E. (2000) Repair of chromosomal abasic sites *in vivo* involves at least three different repair pathways. *EMBO J.*, **19**, 5542–5551.
16. Bohr,V.A., Smith,C.A., Okumoto,D.S. and Hanawalt,P.C. (1985) DNA repair in an active gene: removal of pyrimidine dimers from the DHFR gene of CHO cells is much more efficient than in the genome overall. *Cell*, **40**, 359–369.
17. You,H.J., Swanson,R.L., Harrington,C., Corbett,A.H., Jinks-Robertson,S., Senturker,S., Wallace,S.S., Boiteux,S., Dizdaroglu,M. and Doetsch,P.W. (1999) *Saccharomyces cerevisiae* Ntg1p and Ntg2p: broad specificity *N*-glycosylases for the repair of oxidative DNA damage in the nucleus and mitochondria. *Biochemistry*, **38**, 11298–11306.
18. Meadows,K.L., Song,B. and Doetsch,P.W. (2003) Characterization of AP lyase activities of *Saccharomyces cerevisiae* Ntg1p and Ntg2p: implications for biological function. *Nucleic Acids Res.*, **31**, 5560–5567.
19. Sambrook,J. and Russell,D. (2001) *Molecular Cloning: A Laboratory Manual*. Cold Spring Harbor Laboratory Press, Cold Spring Harbor, NY.
20. O'Rourke,T.W., Doudican,N.A., Mackereth,M.D., Doetsch,P.W. and Shadel,G.S. (2002) Mitochondrial dysfunction due to oxidative mitochondrial DNA damage is reduced through cooperative actions of diverse proteins. *Mol. Cell. Biol.*, **22**, 4086–4093.
21. Bohr,V.A. and Okumoto,D.S. (1988) *Analysis of pyrimidine dimers in defined genes*. In: Friedberg,E.C. and Hanawalt,P.C. (eds.), *DNA Repair: A Laboratory Manual of Research Procedures*. Marcel Dekker, NY, Vol. 3, pp. 347–366.
22. Grubbs,F.E. (1969) Procedure for detecting outlying observations in samples. *Technometrics*, **11**, 1–24.
23. Schmitt,M.E., Brown,T.A. and Trumpower,B.L. (1990) A rapid and simple method for preparation of RNA from *Saccharomyces cerevisiae*. *Nucleic Acids Res.*, **18**, 3091–3092.
24. Eisen,M.B., Spellman,P.T., Brown,P.O. and Botstein,D. (1998) Cluster analysis and display of genome-wide expression patterns. *Proc. Natl Acad. Sci. USA*, **95**, 14863–14868.
25. Qi,H., Li,T.K., Kuo,D., Nur,E.K.A. and Liu,L.F. (2003) Inactivation of Cdc13p triggers MEC1-dependent apoptotic signals in yeast. *J. Biol. Chem.*, **278**, 15136–15141.
26. Leroy,C., Mann,C. and Marsolier,M.C. (2001) Silent repair accounts for cell cycle specificity in the signaling of oxidative DNA lesions. *EMBO J.*, **20**, 2896–2906.
27. Del Carratore,R., Della Croce,C., Simili,M., Taccini,E., Scavuzzo,M. and Sbrana,S. (2002) Cell cycle and morphological alterations as indicative of apoptosis promoted by UV irradiation in *S.cerevisiae*. *Mutat. Res.*, **513**, 183–191.
28. Madeo,F., Frohlich,E., Ligr,M., Grey,M., Sigrist,S.J., Wolf,D.H. and Frohlich,K.U. (1999) Oxygen stress: a regulator of apoptosis in yeast. *J. Cell. Biol.*, **145**, 757–767.
29. Laun,P., Pichova,A., Madeo,F., Fuchs,J., Ellinger,A., Kohlwein,S., Dawes,I., Frohlich,K.U. and Breitenbach,M. (2001) Aged mother cells of *Saccharomyces cerevisiae* show markers of oxidative stress and apoptosis. *Mol. Microbiol.*, **39**, 1166–1173.
30. van den Boom,V., Jaspers,N.G. and Vermeulen,W. (2002) When machines get stuck—obstructed RNA polymerase II: displacement, degradation or suicide. *Bioessays*, **24**, 780–784.
31. Evert,B.A., Salmon,T.B., Song,B., Liu,J.J., Siede,W. and Doetsch,P.W. (2004) Spontaneous DNA damage in *Saccharomyces cerevisiae* elicits phenotypic properties similar to cancer cells. *J. Biol. Chem.*, **279**, 22585–22594.
32. Gasch,A.P., Spellman,P.T., Kao,C.M., Carmel-Harel,O., Eisen,M.B., Storz,G., Botstein,D. and Brown,P.O. (2000) Genomic expression programs in the response of yeast cells to environmental changes. *Mol. Bio. Cell*, **11**, 4241–4257.
33. Causton,H.C., Ren,B., Koh,S.S., Harbison,C.T., Kanin,E., Jennings,E.G., Lee,T.I., True,H.L., Lander,E.S. and Young,R.A. (2001) Remodeling of yeast genome expression in response to environmental changes. *Mol. Bio. Cell*, **12**, 323–337.
34. Reardon,J.T., Bessho,T., Kung,H.C., Bolton,P.H. and Sancar,A. (1997) *In vitro* repair of oxidative DNA damage by human nucleotide excision repair system: possible explanation for neurodegeneration in xeroderma pigmentosum patients. *Proc. Natl Acad. Sci. USA*, **94**, 9463–9468.
35. Snowden,A., Kow,Y.W. and Van Houten,B. (1990) Damage repertoire of the *Escherichia coli* UvrABC nuclease complex includes abasic sites,

base-damage analogues, and lesions containing adjacent 5′ or 3′ nicks. *Biochemistry*, **29**, 7251–7259.
36. Torres-Ramos,C.A., Johnson,R.E., Prakash,L. and Prakash,S. (2000) Evidence for the involvement of nucleotide excision repair in the removal of abasic sites in yeast. *Mol. Cell. Biol.*, **20**, 3522–3528.
37. Tishkoff,D.X., Filosi,N., Gaida,G.M. and Kolodner,R.D. (1997) A novel mutation avoidance mechanism dependent on *S.cerevisiae* RAD27 is distinct from DNA mismatch repair. *Cell*, **88**, 253–263.
38. Jinks-Robertson,S. and Petes,T.D. (1993) Experimental determination of rates of concerted evolution. *Methods Enzymol.*, **224**, 631–646.
39. Finkel,T. (1998) Oxygen radicals and signaling. *Curr. Opin. Cell. Biol.*, **10**, 248–253.
40. Brooks,P.J., Wise,D.S., Berry,D.A., Kosmoski,J.V., Smerdon,M.J., Somers,R.L., Mackie,H., Spoonde,A.Y., Ackerman,E.J., Coleman,K. *et al.* (2000) The oxidative DNA lesion 8,5′-(*S*)-cyclo-2′-deoxyadenosine is repaired by the nucleotide excision repair pathway and blocks gene expression in mammalian cells. *J. Biol. Chem.*, **275**, 22355–22362.
41. Alseth,I., Eide,L., Pirovano,M., Rognes,T., Seeberg,E. and Bjoras,M. (1999) The *Saccharomyces cerevisiae* homologues of endonuclease III from *Escherichia coli*, Ntg1 and Ntg2, are both required for efficient repair of spontaneous and induced oxidative DNA damage in yeast. *Mol. Cell. Biol.*, **19**, 3779–3787.
42. Elledge,S.J., Zhou,Z., Allen,J.B. and Navas,T.A. (1993) DNA damage and cell cycle regulation of ribonucleotide reductase. *Bioessays*, **15**, 333–339.
43. Feig,D.I., Reid,T.M. and Loeb,L.A. (1994) Reactive oxygen species in tumorigenesis. *Cancer Res.*, **54**, 1890s–1894s.
44. Toyokuni,S., Okamoto,K., Yodoi,J. and Hiai,H. (1995) Persistent oxidative stress in cancer. *FEBS Lett.*, **358**, 1–3.